Published in final edited form as:

Curr Biol. 2018 July 09; 28(13): 2007–2017.e4. doi:10.1016/j.cub.2018.04.064.

Reconfiguration of a multi-oscillator network by light in the *Drosophila* circadian clock

Abhishek Chatterjee[1], **Angélique Lamaze**[1,†], **Joydeep De**[1], **Wilson Mena**[1,‡], **Elisabeth Chélot**[1], **Béatrice Martin**[1], **Paul Hardin**[2], **Sebastian Kadener**[3], **Patrick Emery**[4], and **François Rouyer**[1,*]

[1]Institut des Neurosciences Paris-Saclay, Univ. Paris Sud, CNRS, Université Paris-Saclay, 91190 Gif-sur-Yvette, France

[2]Department of Biology and Center for Biological Clocks Research, Texas A&M University, College Station, Texas 77845-3258, U.S.A.

[3]Department of Biology, Brandeis University, Waltham, MA 02454, U.S.A.

[4]Department of Neurobiology, University of Massachusetts Medical School, Worcester, Massachusetts 01605, U.S.A.

Summary

The brain clock that drives circadian rhythms of locomotor activity relies on a multi-oscillator neuronal network [1, 2]. In addition to synchronizing the clock with day-night cycles, light also reformats the clock-driven daily activity pattern [3–5]. How changes in lighting conditions modify the contribution of the different oscillators to remodel the daily activity pattern remains largely unknown. Our data in *Drosophila* indicate that light readjusts the interactions between oscillators through two different modes. We show that a morning s-LNv > DN1p circuit works in series whereas two parallel evening circuits are contributed by LNds and other DN1ps. Based on the photic context, the master pacemaker in the s-LNv neurons swaps its enslaved partner-oscillator - LNd in the presence of light or DN1p in the absence of light - to always link up with the most influential phase-determining oscillator. When exposure to light further increases, the light-activated LNd pacemaker becomes independent by decoupling from the s-LNvs. The calibration of coupling by light is layered on a clock-independent network interaction wherein light upregulates the expression of the PDF neuropeptide in the s-LNvs, which inhibits the behavioral output of the DN1p evening oscillator. Thus, light modifies inter-oscillator coupling and clock-independent

*Corresponding author and lead contact: rouyer@inaf.cnrs-gif.fr.
†Present address: UCL Institute of Neurology, London, U.K
‡Present address: CIRB, Collège de France, Paris, France

Author contributions

A.C. and F.R. designed the project. A.C., A.L., W.M., J.D., E.C. and B.M. designed and performed the experiments. P.H., S.K. and P.E. provided unpublished material. A.C. and F.R. wrote the manuscript with input from A.L., J.D., P.H. and P.E.

Declaration of Interests

The authors declare no competing interests.

output-gating to achieve flexibility in the network. It is likely that the light-induced changes in the *Drosophila* brain circadian network could reveal general principles of adapting to varying environmental cues in any neuronal multi-oscillator system.

eTOC Blurb

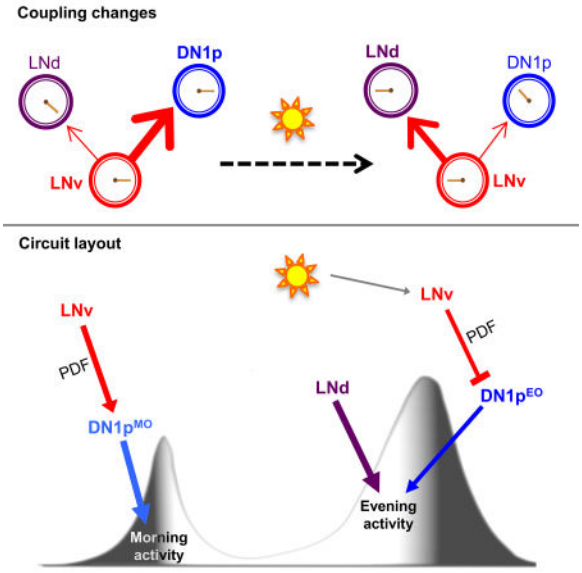

Chatterjee *et al.*, show that light modifies inter-oscillator coupling and clock-independent output-gating in the Drosophila brain clock network. This dynamic flexibility in the interactions among the different oscillator nodes, in part defined by the neuropeptide PDF, allow the hardwired clock network to balance robustness with adaptability.

Keywords

Circadian clock; Drosophila; oscillator coupling; rest-activity rhythms; light; visual system; Pigment-Dispersing Factor

Introduction

Circadian clocks align our physiology and behavior to the 24h day-night cycles that are imposed by the rotation of the earth. The daily rhythm in rest-activity behavior is sculpted by a coupled multi-oscillator system that is located in the brain of both insects [1, 6, 7] and mammals [2, 8]. The circadian clock functions to anticipate daily environmental changes. On the other hand, clock properties are tuned by the environment. Light is the main cue for synchronizing circadian clocks with day-night cycles (entrainment) and a large body of work has investigated light-induced phase shifts [9, 10]. The effects of light on the pace, internal coherence or outputs of circadian oscillators are much less understood [11–19]. We have used the relatively simple clock network of the Drosophila brain to study how flexible interactions among multiple oscillators allows the circadian clock to express behavioral plasticity in face of environmental changes.

Eukaryotic circadian clocks rely on interlocked molecular feedback loops, in which transcription factors activate the expression of their own inhibitors [20]. In Drosophila, the CLOCK/CYCLE complex activates the transcription of the *period (per)* and *timeless (tim)* genes in the evening. PER and TIM proteins slowly accumulate to peak around the end of the night, their stability, subcellular localization and transcriptional function being temporally regulated to generate a 24h oscillation. This regulation largely relies on post-translational mechanisms that involve a series of kinases such as DOUBLE-TIME (DBT), CASEIN KINASE 2 (CK2), SHAGGY (SGG), as well as phosphatases and ubiquitin ligases [20, 21]. Such components thus play a key role in setting the pace of the oscillator. The molecular clockwork maintains synchrony with the external light-dark cycles via the blue-light-sensitive photoreceptor CRYPTOCHROME (CRY) that is expressed in most clock cells and resets the molecular oscillator by triggering the light-induced degradation of TIM, and the Rhodopsin-mediated visual input-pathways [21, 22].

Fruit flies are crepuscular animals displaying morning and evening peaks of activity in light-dark cycles. The circadian clock that underlies this bimodal activity rhythm resides in 150 clock neurons that comprise a series of brain oscillators [1, 7, 23]. Among those, morning and evening oscillators were defined as the small ventral lateral neurons (s-LNvs) that express the Pigment-dispersing factor (PDF) neuropeptide (LN^{MO}) and the four CRY-positive, PDF-negative lateral neurons (3 LNds and 5^{th} s-LNv = LN^{EO}), respectively [15, 24–26]. Not surprisingly, the simplistic idea of separable anatomical substrates for the dual morning/evening oscillators has been questioned by recent findings suggesting that other clock neurons subsets contribute to morning and/or evening activity [14, 27–30]. In particular, a subset of posterior dorsal neurons (DN1ps) can drive both morning and evening activity peaks, with high levels of light inhibiting the evening component [18, 31]. To understand how LNs and DNs interact with light to build locomotor behavior, we sought to analyze how light affects the coupling between oscillators, as coupling has been proposed to be a favorable substrate for translating light's effects on circadian clock properties [11]. Our data reveals reorganization of the fly clock network between different configurations, which are defined by light.

Results

LN^{MO} > DN1p coupling organizes behavioral rhythms in DD

The LN^{MO} is sufficient for behavioral rhythms in constant darkness (DD) whilst the PDF(−) oscillators are not [18, 24, 25]. Moreover, the LN^{MO} clock is necessary for rhythm generation and period determination whereas the clock located in the PDF(−) neurons is not [29, 32, 33] (Figure S1A–B and Table S1). We observed that the behavioral phase, which is defined by previous entrainment, was either delayed or advanced, according to the speed of the molecular oscillator running in the LN^{MO} or DN1ps (Figure 1A and Table 1). In contrast, no change was observed in flies with the same molecular alterations imposed upon the LN^{EO} (Figure 1A and Table 1). In the absence of light, behavioral phase is thus contributed by the DN1ps but not by the LN^{EO}. Interestingly, CRY(+) DN1ps also showed by far the strongest coupling to the LN^{MO} master clock in DD. In flies having either a faster (~22 h period) or a slower (~26 h) clock in the LN^{MO} (Figure 1B, Figure S2A and Table 1),

the DN1p clock readily abandoned its intrinsic 24 h period to follow the speed of the LN^{MO} pacemaker. In comparison, the different subsets of LN^{EO} and other PDF(−) oscillators only showed modest change of their pace (Figure 1B, Figure S2B). When the DN1p oscillator was forced to run faster, the pace of the LN^{MO} remained unaffected (Figure S2C and Table 1), indicating that a hierarchical relationship defines the LN^{MO} > DN1p interaction. Thus, in the absence of light, LN^{MO} sets the period and enslaves DN1ps that contribute to phase determination (Figure 1C).

Light changes coupling and favors a LN^{MO} > LN^{EO} axis to control behavior in LD

We then tested the organization of the clock network in the presence of light. We first used light-dark (LD) 12:12 cycles with moderate (50 lux) light intensity, because they allow both the LN^{EO} and DN1p oscillators to produce evening output [18]. Accelerating the LN^{EO} strongly advanced evening activity whereas changing the pace of the DN1p clock did not affect the evening activity, which normally peaked at the lights-OFF transition (Figure 2A and Figure S3A). Thus, LN^{EO} and not DN1ps set the phase of the evening activity in LD. We then assessed coupling between the LN^{MO} and PDF(−) oscillators, using conditions that favor the hierarchical ascendancy of the LN^{MO}: short photoperiod (when LN^{MO} has a stronger impact on the timing of the evening peak) [16], and absence of CRY (which causes LN^{MO} to be the principal communicator of light input) [34, 35]. Under these conditions, a slowed down LN^{MO} induced delayed evening activity and delayed TIM oscillations in LN^{EO} but not in DN1ps (Figure 2B). Hence, LN^{EO} becomes strongly coupled to LN^{MO} in LD, while coupling between DN1ps and LN^{MO} fades away. Expectedly, absence of PDFR signaling suppressed the LN^{MO}/LN^{EO} coupling (Figure S3B). We thus hypothesized that the light-induced coupling swap between DN1ps and LN^{EO} would be reflected by an opposite effect of light on PDFR signaling in the two slave oscillators. Indeed, CRE-*luc* transcriptional reporter, known to be activated by PDFR-signaling *in vitro* [36, 37], showed higher activity in the LN^{EO} in LD as well as in the DN1ps in DD (Figure 2C). Furthermore, a decreased calcium response in the DN1ps was elicited by bath-application of PDF in LD, in comparison to DD, suggesting that darkness increases their response to PDF (Figure 2C). Taken together, the behavioral, physiological and molecular data indicate that in the presence of moderate light LD cycles, LN^{MO} enslaved LN^{EO} and these coupled LN oscillators determine the phase of the evening activity (Figure 2A–B), while in DD LN^{MO} enslaved the DN1ps. Therefore, we show that light changes the strength of the coupling between PDF(+) LN^{MO} cells and different PDF(−) oscillators to select the most influential slave oscillator.

Interestingly, flies with a long period in the LN^{MO} failed to exhibit a protracted evening peak in high-light intensity LD cycles (Figure S3C, see also [35]). This weakening of LN^{MO} > LN^{EO} coupling in the presence of brighter light (1000 lux) was accompanied by an increasing dominance of the LN^{EO} in defining the network's behavioral output. LN^{EO} indeed ultimately ascend up to determining the pace of the free-running behavioral rhythms in constant light (LL) (Table S1, see also [34]). Thus, the LN^{MO} > LN^{EO} coupling progressively fades away under increasing light exposure (intensity or duration), thereby allowing the LN^{EO} to autonomously set the pace of the behavioral program (Figure 2D).

Morning and evening peaks of activity map to separate DN1p subsets

A clock only in the DN1ps is sufficient to produce both morning and evening peaks in low light conditions [18], raising the question whether the DN1ps could be bifunctional oscillators or contain distinct morning and evening subsets. Heterogeneity of the DN1p neurons is underscored by the differential expression of CRY [18, 26], PDFR [38] and VGLUT (VESICULAR GLUTAMATE TRANSPORTER) [27, 39, 40]. Most CRY(+) DN1ps co-expressed *VGlut* and the *VGlut(−)* DN1ps lacked CRY protein (Figure 3A and Figure S4B). Interestingly, the CRY(−) DN1ps lacked two prominent dendritic projections, which were observed with the CRY(+) DN1ps (Figure 3B), supporting the idea that the two subsets belong to different circuits. An oscillator in the CRY(−) or *VGlut(−)* DN1ps is sufficient only for evening anticipation, in contrast, oscillator restricted to a subset of the *VGlut(+)* DN1ps is sufficient for the morning but not evening anticipation (Figure 3A, C and Figure S4A, C). To address the role of PDF signaling in the behavior that is driven by the DN1p clock, we tested Pdf^{01} mutant flies bearing oscillators in DN1ps only. Such flies had evening but not morning anticipation (Figure 4A). The data thus support the hypothesis that two different subsets of DN1p oscillators control morning and evening behavior, with PDF signaling only required in the morning one. However, we cannot exclude the possibilities that certain DN1ps may produce both the morning and evening peaks, or that within a particular subset further functional heterogeneity might be present.

Distinct logic of organization of morning and evening oscillators

Since morning activity relies on PDF and a clock in either LN^{MO} or CRY(+) $DN1p^{MO}$, we asked how the two morning oscillators interact. Flies that lacked LN^{MO} cells but retained PDFR signaling in the DN1ps through restricted expression of membrane-tethered *t*-PDF displayed morning activity (Figure 4A). Although multiple signals are released by LN^{MO} [41–43], the DN1p oscillator thus requires only PDF for generating morning activity, and the PDF cue does not even need to cycle (see also [44, 45]). However, more complex LNv-derived signals could affect DN1ps in a more natural situation. Our results additionally suggest that feedback from DN1ps to LN^{MO} is dispensable for morning activity. In contrast, flies in which the DN1ps are silenced by targeted expression of the Kir channel show no morning anticipation, indicating that the LN^{MO} requires electrically active DN1p neurons (Figure 4A). Hence, although the LN^{MO} and DN1p oscillators can each generate LD morning activity autonomously, they define a LN^{MO} to DN1p feedforward circuit that relies on clock-independent PDF signaling. Since a clock in either LN^{EO} or CRY(−) $DN1p^{EO}$ can generate evening activity in low light LD, we asked whether the two evening oscillators were acting in series as the morning oscillators were. Ablating most clock cells except the LN^{EO} or DN1ps abolished the morning peak but preserved evening anticipation (Figure 4B and Figure S4D). We conclude that LN^{EO} and DN1p neurons can control evening activity in the absence of another clock neuron relay. Thus, in contrast to the morning circuit contributed by two oscillators that work in series, evening behavior is controlled by two oscillators working in parallel (Figure 4C), allowing independent tuning of their output.

Gating of the DN1p evening output by light relies on PDF signaling

The evening output of the DN1ps is inhibited in high light LD cycles [18]. We first asked which light-input pathway was responsible for this inhibition. The effect of strong light persisted in the absence of CRY but not when photoreceptor cells were silenced by expression of the dominant negative SHIBIRE protein (Figure 5A, Figure S5A). Flies ablated for the extra-retinal Hofbauer-Büchner eyelet (in addition to RH5-expressing retinal photoreceptors) still showed suppression of evening activity (Figure S5B), suggesting that the compound eyes were responsible for the light-induced inhibition of the DN1p-made evening peak. Since PDF is required for visual light input to entrain the DN1ps [34], we asked whether this requirement extends to this novel visually-gated photic inhibition. A strong DN1p-made evening peak persisted under bright light in the absence of PDFR (Figure 5B) or PDF (Figure S6A). This peak was also observed in heterozygous Pdf^{01}/Pdf^{+} flies (Figure 5B, Figure S5A), indicating that high levels of PDF are required for the light-dependent inhibition. Importantly, PDF had little effect on the molecular clockwork of the DN1p oscillators under LD cycles (Figure S6A). The inhibition of the evening peak was reinstalled by either rescuing PDFR in the DN1p evening subset of $Pdfr^{-}$ mutants, or by enhancing PDF levels in only the s-LNvs of Pdf^{01}/Pdf^{+} flies (Figure 5B, Figure S5A), supporting the existence of a direct s-LNv to DN1p pathway for conveying light information. Thus, in addition to setting free the first evening oscillator (LN^{EO}) (Table S1), bright light inhibits the output of the second evening oscillator in the DN1ps through PDF.

How does PDF signaling inhibit the behavioral output of the evening DN1ps? PDF has been shown to increase the firing rate of DN1p neurons [46]. When we chemogenetically activated the LN^{MO} cells and recorded GCaMP6 signal from the DN1ps (Figure 5C), a majority of the DN1p soma indeed elicited depolarizing response (see Figure 2C), but a smaller fraction of the DN1ps displayed a drop of calcium levels consistent with suppression of neuronal activity. Bath-application of PDF similarly revealed two populations – the majority showing a calcium rise evoked by PDF and a sizeable minority displaying a pronounced slump in GCaMP6 signal triggered by PDF (Figure 5C). Bioluminescence-based calcium imaging with a GFP-aequorin fusion reporter [47], upon bath-application of PDF, also revealed calcium rise when the reporter was driven in all DN1ps, but notably a downturn in signal was detected when the reporter was restricted to the non-glutamatergic $DN1p^{EO}$ cells (Figure S6D). Although we cannot exclude that this new high-light–PDF pathway activates DN1ps to trigger a downstream inhibitory circuit, the simplest interpretation of our data is that it inhibits the physiological output of some non-glutamatergic DN1ps to suppress evening activity.

Pdf transcription encodes ambient light intensity

How could PDF encode the light message? We observed that brighter light intensity correlated with increased levels of the BRUCHPILOT (BRP) protein (Figure 6A), which reflects the activity of the LN^{MO} neurons [48, 49]. This was supported by the Calcium-dependent transcriptional reporter of neural activity CaLexA, which revealed stronger LN^{MO} activity under high light intensity (Figure 6A). In agreement with the behavioral results, the high-light-induced neuronal activity of the LN^{MO} was associated with increased levels of PDF immunoreactivity in its soma and axonal arbor (Figure 6B). However, no change was

observed in the arbor's morphology (Figure S6B), whose circadian cycling might promote structural reorganization of the LNv output circuitry on a daily basis [49–51].

The immediate early gene *Hr38* is induced by neural activity and exposure to a light pulse [52, 53] and is expressed in the LN^{MO} [54]. Since HR38 regulates PDF expression through different pathways [55], we asked whether it was involved in the high-light-induced PDF increase. Downregulation of *Hr38* in the LN^{MO} blocked the light-induced increase of PDF levels in the axon terminals (Figure 6C). The higher PDF levels in the terminals did not merely stem from increased transport of the peptide (Figure 6B and Figure S6C). We thus asked whether HR38 could control *Pdf* transcription by using the *Pdf-nls:Tomato:PEST* reporter [55]. *Pdf* transcription was increased by high light and this increase was blocked by downregulating *Hr38* (Figure 6C). Importantly, *Hr38* downregulation in LN^{MO} restored DN1p-generated evening activity in high light LD cycles (Figure 6D). We conclude that the suppression of the DN1p evening output by high light is achieved through a HR38-dependent increase of PDF expression in the LN^{MO}. PDF thus controls the output of the two evening oscillators in LD cycles: in addition to phasing calcium oscillations in the LN^{EO} [19, 56], PDF gates the light-dependent contribution of the DN1ps.

Discussion

Because the individual day-night cycles vary predictably as well as chaotically with respect to most of the cycling cues – light intensity and spectral quality, temperature, etc., it is imperative for a hardwired clock network to balance robustness with adaptability. Here we showed that dynamic flexibility in the hierarchical interactions amongst the different oscillator nodes, in part defined by network-intrinsic peptide neuromodulation, accounts for an element of the required adaptability. We previously showed that between LN morning and evening oscillators, which one drives behavioral rhythms under free-running conditions, is determined by light [15]. In addition, high levels of light suppress the evening peak that is controlled by a clock in the DN1ps in LD conditions [18]. Our study shows that light guides the choice of the most influential follower oscillator via recalibration of its coupling strength with the master oscillator that is located in the PDF-expressing LN^{MO} neurons, the only oscillator that can drive rhythmic behavior in the absence of light cues. PDF(+) neurons also play a role in transmitting visual inputs or non-cell-autonomous CRY signals to synchronize PDF-negative oscillators [57–61]. We show here that a light-induced increase of PDF in the LN^{MO} suppresses the evening output of the DN1ps.

Our data support a model where at least two different pairs of oscillators can autonomously drive morning and evening activity, with each oscillator pair generating only one of the two activity peaks. Whereas a single LN^{MO} > CRY(+) $DN1p^{MO}$ axis generates morning activity, two rather independent circuits headed by either LN^{EO} or CRY(−) $DN1p^{EO}$ generate evening activity, possibly reflecting the importance of the evening peak and its modulation by light in the *Drosophila* activity profile. In addition to generating free running rhythms in the absence of light, the LN^{MO} plays a unique role in the network in LD by leading the morning circuit [24, 25, 31, 34, 62] and strongly influencing the LN^{EO}, hence the evening activity [19, 30, 34, 35, 62, 63]. Our results reveal that light intensity controls the coupling between the LN^{MO} and LN^{EO}, from weak in the absence of light to strong with moderate

amounts of light, while still higher light levels diminishing it again. The light-induced increase of the LN^{MO} > LN^{EO} coupling goes with a decrease of the LN^{MO} > DN1p coupling, which is strong in the dark.

Under natural conditions, in the second half of the daytime when luminance is high, the LN^{EO} would autonomously control the onset of evening activity in high light and then become progressively coupled with the LN^{MO} as light levels decrease in the evening. At night, the LN^{MO} would switch its coupling from LN^{EO} to DN1p, in particular $DN1p^{MO}$ to prepare building morning activity to which the LN^{EO} does not contribute. The loss of only the morning activity, and not the evening activity, in flies with a clock only in the DN1ps but no PDF also suggests the existence of a LN^{MO}-coupled $DN1p^{MO}$ and a more autonomous $DN1p^{EO}$. PDF levels show daily cycles with a peak in the morning [64, 65]. Thus, the LN^{MO} > LN^{EO} coupling, which is strong in low light, may rely on low PDF levels in the evening, whereas high light earlier in the day would decrease the sensitivity of the LN^{EO} to PDF. This would be in agreement with recent data showing that PDF strongly delays calcium oscillations in the LNds in DD whereas a much weaker delay is observed in LD [19]. It thus appears that high light can mask the action of PDF on the CRY-expressing LN^{EO} neurons. In the same line, the effect of PDF on the phase of the LN^{EO}-driven evening peak in LD is much stronger in the absence of CRY [34, 35, 63]. Since downstream mediators of PDFR signaling are regulated by light [66], it will be interesting to see whether light affects this signaling pathway differently in the different subsets of PDFR-expressing neurons. The present results show that light-induced increase of PDF levels, inhibits the behavioral output of the CRY-negative $DN1p^{EO}$ neurons, which also have low PDFR expression [38]. Light could thus either increase PDF action on weakly responding cells (e.g. $DN1p^{EO}$) or decrease it on strongly responding cells (e.g. LN^{EO}). Under natural conditions, decrease in light intensity and PDF levels at the end of the day would thus disinhibit the output of the $DN1p^{EO}$ in addition to reinforcing the LN^{MO} > LN^{EO} coupling.

The strong plasticity of the *Drosophila* diurnal behavior thus appears to rely on specialized oscillators, with light and light-modulated PDF levels largely defining their weight and coupling over the course of a day. It will be interesting to analyze how modulation of coupling and output by light intensity and PDF contribute to the behavioral adaptation to seasonal changes of photoperiod. Scalability of coupling is thought to favor adaptation to environmental changes as shown in the mammalian suprachiasmatic nuclei (SCN) [17]. Like PDF in flies, the vasoactive intestinal peptide (VIP) plays a key role in transmitting light information from the ventral SCN to the dorsal one [2, 67]. It is not known whether light increases VIP levels, but high VIP reduces synchrony between SCN neurons and speeds up entrainment to LD cycles [68]. Whether light and VIP also reorganize SCN circuits by switching coupling from one population to another or by inhibiting the output of specific neuronal populations remains to be determined.

STAR Methods

CONTACT FOR REAGENT AND RESOURCE SHARING

Further information and requests for resources and reagents should be directed to and will be fulfilled by the Lead Contact, François Rouyer (rouyer@inaf.cnrs-gif.fr).

EXPERIMENTAL MODEL AND SUBJECT DETAILS

Rearing of Drosophila—All strains were reared on corn meal media at 25°C in 12-12 LD conditions.

Fly strains—*cry*^{b} [72], *cry*^{0} [73], *Pdf*^{01} [62], *Pdfr*^{han5304} [74], *per*^{0} [75], *Pdf-Gal4* [62], *Clk4.1M-Gal4* [18], *Mai179-Gal4* [76], *tim(UAS)-Gal4* [77], *Clock*^{6939}*-Gal4* [78], *cry-Gal4(19)* [15], *cry-Gal4(13)* [79], *Clk-int1-3-Gal4(9M)* [80], *Gal1118* [32], *Rh5-Gal4* [81], *OK371(VGlut)-Gal4* [82], *Pdf-Gal80* and *cry-Gal80* [25], *VGlut-Gal80* [83], *VGlut*^{MI04979}*-Gal80* [84], *UAS-per16* [32], *UAS-cyc*^{DN} [85], *UAS-dbt*^{S} [86], *UAS-CkIIα* ^{Tik} [87], *UAS-dti* [88], *UAS-CaLexA* [89], *UAS-brp:gfp* [90], *UAS-DenMark,UAS-syt:gfp* [91], *UAS-sgg*^{S9A} [92], *UAS-Kir* [93], *UAS-Hr38-miRNA* [94], *UAS-GCaMP6s* [95], *Pdf-LexA* [97], *Clk4.1MLexA* [98], *LexAop-P2X*$_{2}$ [99] *GMR-shi*^{K39A} [100], *Rh6-GFP* [102], *Pdf-DTI* [101], *20xUASaeq: gfp* [47, 105] and *UAS-tPDF* lines [37, 106] were previously described. *UAS-cd8::gfp, UAS-gfp*^{S65T}*, UAS-nls::gfp, Tub-FRT-stop-FRT-Gal80, tub-Gal80*^{ts}*, GMR18H11-LexA, LexAop-nls:mCherry, LexAop-Gal80,* were ordered from the Bloomington stock center (U.S.A), while the *VT027231-Gal4 line was from the VDRC stock center* (Austria) *and the UAS-CkIIα-RNAi* (17520R2) was from NIG (Japan). *Clk4.1M-Gal80* is *LexAop-Gal80; Clk4.1M-LexA* and *ITP-Gal80* is *ITP-flp*$_{o}$*; tub-FRT-stop-FRT-Gal80. DenMark* (mouse *Icam5* fused to *mCherry*) labels the somatodendritic compartments and *syt:gfp* the presynaptic terminals of neurons. *CRE-F-luc* allows Flp/FRT recombination-based cell-specific recording of CRE-reporter activity [103]. *Pdf-nls.Tomato:PEST* allows short-lived, nuclear-localized, fluorescent readout of *Pdf* gene transcription [55]. Readers are referred to Table 1 of reference [60] for summary of expression pattern of most of the key *Gal4* lines used in our study. In addition, the clock neurons that express the different *Gal4* (based on GFP staining) are indicated in the Key Resources Table.

METHOD DETAILS

Generation of transgenic flies—The *LexAop-per* construct was generated by PCR amplifying the 3.9 kb *per* cDNA [32] with the following primers: 5'-aaactcgagACTAGTCAACCAACTGGGCAAG-3' and rev 5'aaatctagaGAAGAACTTGAAGGGAATGGAA-3'. This fragment was cloned in *pJFRC19-13XLexAop2-IVS-myr ::gfp* (Addgene #26224) using XhoI and XbaI sites, which eliminated the *myr ::gfp* sequence. After confirmation by sequencing, the construct was introduced into VK00033 flies by PhiC31 integrase mediated transgenesis (BestGene). *w; Itp-flp*$_{o}$ flies were obtained by Recombinase Mediated Cassette Exchange [107]: the MiMIC insertion Mi{MIC}ITP^{MI00349} present in BDSC stock #30713 was replaced by the FLPo ORF sequence using a DGRC vector (stock #1326) via injection of the donor plasmid (BestGene).

Behavioral analysis—Experiments were carried out with 3–5 day old adult males, raised under high light conditions at 25°C, in *Drosophila* activity monitors (TriKinetics) as previously described [108]. In the incubators, light intensity was about 1000 lux (at 555 nm), which we designate as high light. To cut off light intensity to 50 lux we added grey neutral-density filters to the monitors. Light spectra and irradiance were measured with a USB200

(Ocean Optics) spectrometer. For DD analysis, flies were first entrained in 12 h:12 h LD cycles for at least 3 days (light-ON at 9am, light-OFF at 9pm), and activity data were analyzed for at least 9 days, starting from the second day in DD. Data analysis was done with the FaasX 1.21 software, which is derived from the Brandeis Rhythm Package. FaasX runs on Apple Macintosh OSX and is freely available (http://neuropsi.cnrs.fr/spip.php?article298&lang=en). Bin size was 30 minutes. Rhythmic flies were defined by autocorrelation and chi-square periodogram analysis with the following criteria respectively; RI jitter =5 bins and maximum lag =144 bins (autocorrelation), filter OFF and power ≥20 and width ≥1.5 h (chi-square periodogram). Power is the height of the periodogram peak and give the significance of the calculated period. Qp/N (=Qp/Qp-max) is a measure of the robustness of the rhythm. The periodogram peak position was based on the maximum Qp bin. Only the highest periodogram peak (tau-1) above the defined significance level ($p<0.05$) was considered for behavioral period calculations. Mean daily activity (number of events per 0.5 h± standard error of the mean [109]) was calculated over the whole period of DD. The chi-square periodogram derived DD phase value (Phase(tau)) was the time at which the trough of activity occurred in DD (relative to a fixed reference point set at midnight) and was averaged from at least 9 days of data from DD day-2 onward. To allow comparisons between genotypes the Phase(tau) value was plotted on a 24h fixed-period clock. See [108] for details of phase analysis. Only rhythmic flies were included in phase analysis. All behavioral experiments were reproduced 2 or 3 times with similar results. For LD 12:12 experiments, locomotor activity profiles were averaged from n flies for 4–5 days leaving out the first couple of days of recordings from quantitative analyses. Activity data registered after 4–5 days of entrainment were included for photoperiods other than 12:12. Each white/grey bar in the 24-hr activity histogram represents mean activity levels in a 0.5h interval during the light phase and black bars represent that during the dark phase of the LD cycle. The Evening peak was the highest activity bin in the second half of the photoperiod. The onset was defined as the starting point of a continuous increase of activity toward the peak, allowing one-step decrease in this duration [45]. The offset was defined as the end point of a continuous decrease of activity after the peak, allowing one-step increase in this duration. Evening concentration was defined as the 6h/12h activity ratio prior to the light-OFF transition and morning anticipation index was calculated from the 3h/6h activity ratio prior to the light-ON transition.

Immunolabelings—All experiments were done on whole-mounted adult brains. guinea-pig anti-CRY serum had been provided by J. Levine and was used at 1:2,000 dilution. The rabbit anti-PER antiserum [69] was used at 1:15,000 dilution. The rat TIM antiserum [70] and the mouse PDF antiserum (Developmental Studies Hybridoma Bank) were used at 1:10,000 and 1:20,000 dilutions, respectively. PAP [62]) at 1:1500, rabbit PDF at 1:10,000, chicken/mouse/rabbit GFP at 1:1000, rabbit dsRed at 1:500, mouse luc at 1:100 were used. Fluorescence signals were analyzed with a Zeiss AxioImager Z1 semiconfocal microscope equipped with a AxioCam MRm digital camera and an apotome with an adjustable grid which provided structured illumination. Fluorescence intensity was quantified from digital images with the ImageJ software. We applied the formula: $I = 100 \times (S-B)/B$, that gives the fluorescence percentage above background (where S is the mean intensity inside the cell, and B is the mean intensity of the region adjacent to the positive cell). Images for clock

protein oscillations were acquired with a 63× objective. Integrated densities over a defined thresholded area of the axonal arbors of the s-LNvs acquired with a 40× objective were analyzed for quantifying signal in the dorsal projection of the PDF neurons.

GCaMP6 imaging—Only one recording was made from a single explanted brain. Adult Flies were dissected under ice-cold AHL [110] for PDF bath-application experiments and under ice-cold HL3 [111] for $P2X_2$ experiments. The whole brain explants were placed on 42 mm diameter coverslips previously treated with Poly-D-Lysine and Laminin. Then the preparation was covered with oxygenated AHL or HL3. Calcium imaging was performed with a Zeiss Axio Examiner D1 upright microscope with Apochromat 40× W NA 1.0 immersion lens. GCaMP6s probe was excited (25ms exposure time) with a Colibri 470 nm LED light source and images were acquired using AxioCam MRm at 0.5–2 Hz sampling rate. 5 mM ATP (Sigma-Aldrich Chemical) was used to stimulate the $P2X_2$ channel. When used, 30–100μM PDF (PolyPeptide) was added after at least a minute of baseline recording. ATP was dissolved in HL3 solution and PDF in 0.1% DMSO in AHL. The average fluorescence of all pixels for each time point in a defined ROI was subtracted from the average background fluorescence of an identically size ROI elsewhere within the brain. The resulting pixel fluorescence value for each time point was defined as trace F_b. Changes in fluorescence were computed as $\%\Delta F/F_0 = ((F_b\text{-}F_0)/F_0) \times 100$, where F_0 is defined as the average background-subtracted baseline fluorescence for the 30–60 frames preceding the stimulus application. All images were processed and quantified using Fiji (Image J). Maximum GCaMP6s fluorescence change values (Max $\Delta F/F_0$) were determined as the maximum percentage change observed for each trace over the entire duration of each imaging experiment. Maximum values for each treatment and genotypes were averaged to calculate the mean maximum change from baseline.

GFP:aequorin live-imaging—Live GFP:aequorin bioluminescence was used to reveal dynamic changes in intracellular calcium levels [47, 112] in view of its advantage of long temporal summation for weak signals. Dissected brains were transferred in Ringer buffer [47] after preincubation in 2 μM native coelenterazine for 90 minutes. Explanted brains were imaged on an Olympus Luminoview microscope with EMCCD camera cooled to −80 °C, 20× water-dipping high NA objective, and 1200× gain setting. To ameliorate the signal-to-noise ratio, data were acquired with 60s integration time. Recordings were carried out at ZT6–9, and a single recording was made from a single brain preparation.

QUANTIFICATION AND STATISTICAL ANALYSIS

Statistical analysis was done with R and Prism (GraphPad). For calculation of the slope of evening anticipation a linearity test using F-statistic was carried out first. Existence of putative association between binned time and activity level preceding light-on/off transition was quantified by the spearman's rank-correlation coefficient (rho) whose significance (at α=0.05) was ascertained by T-test. Characterization of the DD phase vector of a single fly-group was performed by testing for angular uniformity of data by Hodges-Ajne U-test and also testing for the presence of a specified mean direction in the sample by Rayleigh R-test. The non-parametric Watson's U^2 statistic was used to compare whether two groups of principal azimuths from two different genotypes, come from the same distribution or not

(α=0.05). To determine acrophase from 24-hr biochemical (TIM) cycling data, cosinor analysis was used. Fisher's exact test was used for comparing two proportions. Two sample means were compared by unpaired two-tailed t-test with Welch's correction for heteroscedastic dataset and multiple sample means were compared by ANOVA with post-hoc comparison obtained from Tukey's HSD test (α=0.05). For non-normally distributed data, sample means were compared by Mann-Whitney U test.

Supplementary Material

Refer to Web version on PubMed Central for supplementary material.

Acknowledgments

We thank Bloomington, VDRC and NIG *Drosophila* Stock Centers for fly stocks. We thank M. Boudinot for the FaasX software, F. Laudillay for his help with several experiments, T. Manoliu for his expertise with confocal microscopy, P.-L. Ruffault for figure preparation, J.-R. Martin for advice with GFP-Aequorin experiments, Olympus France for allowing us to perform test experiments with the Luminoview microscope and M. Rosbash and M. Schlichting for their comments on a previous version of the manuscript. We acknowledge funding from Agence Nationale de la Recherche (ClockNet, ClockEye and TEFOR grants), Fondation pour la Recherche Médicale (Equipe FRM grant), European Union 6th (EUCLOCK) and 7th (INsecTIME) Framework Program, and Région Ile-de-France (DIM Neuroscience). A.C. was supported by the European Molecular Biology Organization (EMBO), ANR and Ecole des Neurosciences de Paris (ENP), and F.R. by Institut National de la Santé et de la Recherche Médicale (INSERM). P.E. is supported by a MIRA award from the National Institute of General Medicine Sciences (1R35GM118087).

References

1. Beckwith EJ, Ceriani MF. Communication between circadian clusters: The key to a plastic network. FEBS Lett. 2015; 589:3336–3342. [PubMed: 26297822]
2. Evans JA. Collective timekeeping among cells of the master circadian clock. J Endocrinol. 2016; 230:R27–49. [PubMed: 27154335]
3. Duffy JF, Czeisler CA. Effect of Light on Human Circadian Physiology. Sleep Med Clin. 2009; 4:165–177. [PubMed: 20161220]
4. Yoshii T, Rieger D, Helfrich-Forster C. Two clocks in the brain: An update of the morning and evening oscillator model in Drosophila. Prog Brain Res. 2012; 199:59–82. [PubMed: 22877659]
5. Lucas RJ. Mammalian inner retinal photoreception. Curr Biol. 2013; 23:R125–33. [PubMed: 23391390]
6. Stengl M, Werckenthin A, Wei H. How does the circadian clock tick in the Madeira cockroach? Curr Opin Insect Sci. 2015; 12:38–45.
7. Chatterjee, A., Rouyer, F. Control of Sleep-Wake Cycles in Drosophila. In: Sassone-Corsi, P., Christen, Y., editorsA Time for Metabolism and HormonesSpringer; 201671-78
8. Herzog ED, Hermanstyne T, Smyllie NJ, Hastings MH. Regulating the Suprachiasmatic Nucleus (SCN) Circadian Clockwork: Interplay between Cell-Autonomous and Circuit-Level Mechanisms. Cold Spring Harb Perspect Biol. 2017; 9:a027706. [PubMed: 28049647]
9. Daan S. The Colin S. Pittendrigh Lecture. Colin Pittendrigh, Jurgen Aschoff, and the natural entrainment of circadian systems. J Biol Rhythms. 2000; 15:195–207. [PubMed: 10885874]
10. Roenneberg T, Daan S, Merrow M. The art of entrainment. J Biol Rhythms. 2003; 18:183–194. [PubMed: 12828276]
11. Pittendrigh C, Daan S. A Functional analysis of circadian pacemakers in nocturnal rodentsVPacemaker structure: a clock for all seasons. J Comp Physiol A Neuroethol Sens Neural Behav Physiol. 1976; 106:333–335.
12. Aschoff, J. Free Running and Entrained Circadian Rhythms. In: Aschoff, J., editorBiological RhythmsVol. 4. New York: Plenum; 198181-93

13. Yoshii T, Funada Y, Ibuki-Ishibashi T, Matsumoto A, Tanimura T, Tomioka K. Drosophila cry(b) mutation reveals two circadian clocks that drive locomotor rhythm and have different responsiveness to light. J Insect Physiol. 2004; 50:479–488. [PubMed: 15183277]
14. Rieger D, Shafer OT, Tomioka K, Helfrich-Forster C. Functional analysis of circadian pacemaker neurons in Drosophila melanogaster. J Neurosci. 2006; 26:2531–2543. [PubMed: 16510731]
15. Picot M, Cusumano P, Klarsfeld A, Ueda R, Rouyer F. Light activates output from evening neurons and inhibits output from morning neurons in the Drosophila circadian clock. PLoS Biol. 2007; 5:e315. [PubMed: 18044989]
16. Stoleru D, Nawathean P, Fernandez Mde L, Menet JS, Ceriani MF, Rosbash M. The Drosophila circadian network is a seasonal timer. Cell. 2007; 129:207–219. [PubMed: 17418796]
17. Vanderleest HT, Houben T, Michel S, Deboer T, Albus H, Vansteensel MJ, Block GD, Meijer JH. Seasonal Encoding by the Circadian Pacemaker of the SCN. Curr Biol. 2007; 17:468–473. [PubMed: 17320387]
18. Zhang Y, Liu Y, Bilodeau-Wentworth D, Hardin PE, Emery P. Light and Temperature Control the Contribution of Specific DN1 Neurons to Drosophila Circadian Behavior. Curr Biol. 2010; 20:600–605. [PubMed: 20362449]
19. Liang X, Holy TE, Taghert PH. A Series of Suppressive Signals within the Drosophila Circadian Neural Circuit Generates Sequential Daily Outputs. Neuron. 2017; 94:1173–1189.e4. [PubMed: 28552314]
20. Mendoza-Viveros L, Bouchard-Cannon P, Hegazi S, Cheng AH, Pastore S, Cheng HM. Molecular modulators of the circadian clock: lessons from flies and mice. Cell Mol Life Sci. 2017; 74:1035–1059. [PubMed: 27689221]
21. Dubowy C, Sehgal A. Circadian Rhythms and Sleep in Drosophila melanogaster. Genetics. 2017; 205:1373–1397. [PubMed: 28360128]
22. Yoshii T, Hermann-Luibl C, Helfrich-Förster C. Circadian light-input pathways in Drosophila. Commun Integr Biol. 2016; 9:e1102805. [PubMed: 27066180]
23. Hermann-Luibl C, Helfrich-Förster C. Clock network in Drosophila. Curr Opin Insect Sci. 2015; 7:65–70.
24. Grima B, Chélot E, Xia R, Rouyer F. Morning and evening peaks of activity rely on different clock neurons of the Drosophila brain. Nature. 2004; 431:869–873. [PubMed: 15483616]
25. Stoleru D, Peng P, Agosto J, Rosbash M. Coupled oscillators control morning and evening locomotor behavior of *Drosophila*. Nature. 2004; 431:862–868. [PubMed: 15483615]
26. Yoshii T, Todo T, Wulbeck C, Stanewsky R, Helfrich-Forster C. Cryptochrome is present in the compound eye and a subset of Drosophila's clock neurons. J Comp Neurol. 2008; 508:952–966. [PubMed: 18399544]
27. Collins B, Kaplan HS, Cavey M, Lelito KR, Bahle AH, Zhu Z, Macara AM, Roman G, Shafer OT, Blau J. Differentially Timed Extracellular Signals Synchronize Pacemaker Neuron Clocks. PLoS Biol. 2014; 12:e1001959. [PubMed: 25268747]
28. Dissel S, Hansen CN, Ozkaya O, Hemsley M, Kyriacou CP, Rosato E. The logic of circadian organization in Drosophila. Curr Biol. 2014; 24:2257–2266. [PubMed: 25220056]
29. Yao Z, Shafer OT. The Drosophila circadian clock is a variably coupled network of multiple peptidergic units. Science. 2014; 343:1516–1520. [PubMed: 24675961]
30. Yao Z, Bennett AJ, Clem JL, Shafer OT. The Drosophila Clock Neuron Network Features Diverse Coupling Modes and Requires Network-wide Coherence for Robust Circadian Rhythms. Cell Rep. 2016; 17:2873–2881. [PubMed: 27974202]
31. Zhang L, Chung BY, Lear BC, Kilman VL, Liu Y, Mahesh G, Meissner RA, Hardin PE, Allada R. DN1(p) Circadian Neurons Coordinate Acute Light and PDF Inputs to Produce Robust Daily Behavior in Drosophila. Curr Biol. 2010; 20:591–599. [PubMed: 20362452]
32. Blanchardon E, Grima B, Klarsfeld A, Chélot E, Hardin PE, Préat T, Rouyer F. Defining the role of Drosophila lateral neurons in the control of circadian activity and eclosion rhythms by targeted genetic ablation and PERIOD protein overexpression. Eur J Neurosci. 2001; 13:871–888. [PubMed: 11264660]
33. Beckwith EJ, Ceriani MF. Experimental assessment of the network properties of the Drosophila circadian clock. J Comp Neurol. 2015; 523:982–996. [PubMed: 25504089]

34. Cusumano P, Klarsfeld A, Chélot E, Picot M, Richier B, Rouyer F. PDF-modulated visual inputs and Cryptochrome define diurnal behavior in Drosophila. Nat Neurosci. 2009; 12:1427–1433.
35. Zhang L, Lear BC, Seluzicki A, Allada R. The CRYPTOCHROME photoreceptor gates PDF neuropeptide signaling to set circadian network hierarchy in Drosophila. Curr Biol. 2009; 19:2050–2055. [PubMed: 19913424]
36. Mertens I, Vandingenen A, Johnson EC, Shafer OT, Li W, Trigg JS, De Loof A, Schoofs L, Taghert PH. PDF Receptor Signaling in Drosophila Contributes to Both Circadian and Geotactic Behaviors. Neuron. 2005; 48:213–219. [PubMed: 16242402]
37. Choi C, Fortin JP, McCarthy E, Oksman L, Kopin AS, Nitabach MN. Cellular dissection of circadian peptide signals with genetically encoded membrane-tethered ligands. Curr Biol. 2009; 19:1167–1175. [PubMed: 19592252]
38. Im SH, Taghert PH. PDF receptor expression reveals direct interactions between circadian oscillators in drosophila. J Comp Neurol. 2010; 518:1925–1945. [PubMed: 20394051]
39. Hamasaka Y, Rieger D, Parmentier ML, Grau Y, Helfrich-Forster C, Nassel DR. Glutamate and its metabotropic receptor in Drosophila clock neuron circuits. J Comp Neurol. 2007; 505:32–45. [PubMed: 17729267]
40. Guo F, Yu J, Jung HJ, Abruzzi KC, Luo W, Griffith LC, Rosbash M. Circadian neuron feedback controls the Drosophila sleep-activity profile. Nature. 2016; 536:292–297. [PubMed: 27479324]
41. Helfrich-Förster C. The period clock gene is expressed in central nervous system neurons which also produce a neuropeptide that reveals the projections of circadian pacemaker cells within the brain of drosophila melanogaster. Proc Natl Acad Sci U S A. 1995; 92:612–616. [PubMed: 7831339]
42. Johard HA, Yoishii T, Dircksen H, Cusumano P, Rouyer F, Helfrich-Forster C, Nassel DR. Peptidergic Clock Neurons in Drosophila: Ion Transport Peptide and Short Neuropeptide F in Subsets of Dorsal and Ventral Lateral Neurons. J Comp Neurol. 2009; 516:59–73. [PubMed: 19565664]
43. Frenkel L, Muraro NI, Beltrán González AN, Marcora MS, Bernabó G, Hermann-Luibl C, Romero JI, Helfrich-Förster C, Castaño EM, Marino-Busjle C, et al. Organization of Circadian Behavior Relies on Glycinergic Transmission. Cell Rep. 2017; 19:72–85. [PubMed: 28380364]
44. Kula E, Levitan ES, Pyza E, Rosbash M. PDF Cycling in the Dorsal Protocerebrum of the Drosophila Brain Is Not Necessary for Circadian Clock Function. J Biol Rhythms. 2006; 21:104–117. [PubMed: 16603675]
45. Choi C, Cao G, Tanenhaus AK, McCarthy EV, Jung M, Schleyer W, Shang Y, Rosbash M, Yin JC, Nitabach MN. Autoreceptor Control of Peptide/Neurotransmitter Corelease from PDF Neurons Determines Allocation of Circadian Activity in Drosophila. Cell Rep. 2012; 2:332–344. [PubMed: 22938867]
46. Seluzicki A, Flourakis M, Kula-Eversole E, Zhang L, Kilman V, Allada R. Dual PDF signaling pathways reset clocks via TIMELESS and acutely excite target neurons to control circadian behavior. PLoS Biol. 2014; 12:e1001810. [PubMed: 24643294]
47. Martin JR, Rogers KL, Chagneau C, Brulet P. In vivo Bioluminescence Imaging of Ca Signalling in the Brain of Drosophila. PLoS ONE. 2007; 2:e275. [PubMed: 17342209]
48. Gorostiza EA, Depetris-Chauvin A, Frenkel L, Pirez N, Ceriani MF. Circadian Pacemaker Neurons Change Synaptic Contacts across the Day. Curr Biol. 2014; 24:2161–2167. [PubMed: 25155512]
49. Petsakou A, Sapsis TP, Blau J. Circadian Rhythms in Rho1 Activity Regulate Neuronal Plasticity and Network Hierarchy. Cell. 2015; 162:823–835. [PubMed: 26234154]
50. Fernández MP, Berni J, Ceriani MF. Circadian remodeling of neuronal circuits involved in rhythmic behavior. PLoS Biol. 2008; 6:e69. [PubMed: 18366255]
51. Sivachenko A, Li Y, Abruzzi KC, Rosbash M. The transcription factor Mef2 links the Drosophila core clock to Fas2, neuronal morphology, and circadian behavior. Neuron. 2013; 79:281–292. [PubMed: 23889933]
52. Fujita N, Nagata Y, Nishiuchi T, Sato M, Iwami M, Kiya T. Visualization of neural activity in insect brains using a conserved immediate early gene, Hr38. Curr Biol. 2013; 23:2063–2070. [PubMed: 24120640]

53. Adewoye AB, Kyriacou CP, Tauber E. Identification and functional analysis of early gene expression induced by circadian light-resetting in Drosophila. BMC Genomics. 2015; 16:570. [PubMed: 26231660]
54. Chen X, Rahman R, Guo F, Rosbash M. Genome-wide identification of neuronal activity-regulated genes in Drosophila. Elife. 2016; 5:e19942. [PubMed: 27936378]
55. Mezan S, Feuz JD, Deplancke B, Kadener S. PDF Signaling Is an Integral Part of the Drosophila Circadian Molecular Oscillator. Cell Rep. 2016; 17:708–719. [PubMed: 27732848]
56. Liang X, Holy TE, Taghert PH. Synchronous Drosophila circadian pacemakers display nonsynchronous Ca^{2+} rhythms in vivo. Science. 2016; 351:976–981. [PubMed: 26917772]
57. Tang CH, Hinteregger E, Shang Y, Rosbash M. Light-Mediated TIM Degradation within Drosophila Pacemaker Neurons (s-LNvs) Is Neither Necessary nor Sufficient for Delay Zone Phase Shifts. Neuron. 2010; 66:378–385. [PubMed: 20471351]
58. Guo F, Cerullo I, Chen X, Rosbash M. PDF neuron firing phase-shifts key circadian activity neurons in Drosophila. Elife. 2014; 3:e02780.
59. Schlichting M, Menegazzi P, Lelito KR, Yao Z, Buhl E, Dalla Benetta E, Bahle A, Denike J, Hodge JJ, Helfrich-Förster C, et al. A Neural Network Underlying Circadian Entrainment and Photoperiodic Adjustment of Sleep and Activity in Drosophila. J Neurosci. 2016; 36:9084–9096. [PubMed: 27581451]
60. Yoshii T, Hermann-Luibl C, Kistenpfennig C, Schmid B, Tomioka K, Helfrich-Forster C. Cryptochrome-dependent and -independent circadian entrainment circuits in Drosophila. J Neurosci. 2015; 35:6131–6141. [PubMed: 25878285]
61. Eck S, Helfrich-Förster C, Rieger D. The Timed Depolarization of Morning and Evening Oscillators Phase Shifts the Circadian Clock of Drosophila. J Biol Rhythms. 2016; 31:428–442. [PubMed: 27269519]
62. Renn SC, Park JH, Rosbash M, Hall JC, Taghert PH. A pdf neuropeptide gene mutation and ablation of PDF neurons each cause severe abnormalities of behavioral circadian rhythms in Drosophila. Cell. 1999; 99:791–802. [PubMed: 10619432]
63. Im SH, Li W, Taghert PH. PDFR and CRY Signaling Converge in a Subset of Clock Neurons to Modulate the Amplitude and Phase of Circadian Behavior in Drosophila. PLoS One. 2011; 6:e18974. [PubMed: 21559487]
64. Park JH, Helfrich-Förster C, Lee G, Liu L, Rosbash M, Hall JC. Differential regulation of circadian pacemaker output by separate clock genes in Drosophila. Proc Natl Acad Sci U S A. 2000; 97:3608–3613. [PubMed: 10725392]
65. Hermann-Luibl C, Yoshii T, Senthilan PR, Dircksen H, Helfrich-Forster C. The Ion Transport Peptide Is a New Functional Clock Neuropeptide in the Fruit Fly Drosophila melanogaster. J Neurosci. 2014; 34:9522–9536. [PubMed: 25031396]
66. Zhang Y, Emery P. GW182 controls Drosophila circadian behavior and PDF-receptor signaling. Neuron. 2013; 78:152–165. [PubMed: 23583112]
67. Aton SJ, Herzog ED. Come together, right.Now: synchronization of rhythms in a Mammalian circadian clock. Neuron. 2005; 48:531–534. [PubMed: 16301169]
68. An S, Harang R, Meeker K, Granados-Fuentes D, Tsai CA, Mazuski C, Kim J, Doyle FJ, Petzold LR, Herzog ED. A neuropeptide speeds circadian entrainment by reducing intercellular synchrony. Proc Natl Acad Sci U S A. 2013; 110:E4355–61. [PubMed: 24167276]
69. Stanewsky R, Frisch B, Brandes C, Hamblen-Coyle MJ, Rosbash M, Hall JC. Temporal and spatial expression patterns of transgenes containing increasing amounts of the *Drosophila* clock gene *period* and a *lacZ* reporter: mapping elements of the PER protein involved in circadian cycling. J Neurosci. 1997; 17:676–696. [PubMed: 8987790]
70. Grima B, Lamouroux A, Chélot E, Papin C, Limbourg-Bouchon B, Rouyer F. The F-box protein SLIMB controls the levels of clock proteins PERIOD and TIMELESS. Nature. 2002; 429:178–182.
71. Malpel S, Klarsfeld A, Rouyer F. Larval optic nerve and adult extra-retinal photoreceptors sequentially associate with the clock neurons during *Drosophila* brain development. Development. 2002; 129:1443–1453. [PubMed: 11880353]

72. Stanewsky R, Kaneko M, Emery P, Beretta B, Wager-Smith K, Kay SA, Rosbash M, Hall JC. The cryb mutation identifies cryptochrome as a circadian photoreceptor in Drosophila. Cell. 1998; 95:681–692. [PubMed: 9845370]
73. Dolezelova E, Dolezel D, Hall JC. Rhythm Defects Caused by Newly Engineered Null Mutations in Drosophila's cryptochrome Gene. Genetics. 2007; 177:329–345. [PubMed: 17720919]
74. Hyun S, Lee Y, Hong ST, Bang S, Paik D, Kang J, Shin J, Lee J, Jeon K, Hwang S, et al. Drosophila GPCR Han Is a Receptor for the Circadian Clock Neuropeptide PDF. Neuron. 2005; 48:267–278. [PubMed: 16242407]
75. Konopka RJ, Benzer S. Clock mutants in Drosophila melanogaster. Proc Natl Acad Sci U S A. 1971; 68:2112–2116. [PubMed: 5002428]
76. Siegmund T, Korge G. Innervation of the ring gland of Drosophila melanogaster. J Comp Neurol. 2001; 431:481–491. [PubMed: 11223816]
77. Blau J, Young MW. Cycling vrille expression is required for a functional Drosophila clock. Cell. 1999; 99:661–671. [PubMed: 10612401]
78. Gummadova JO, Coutts GA, Glossop NR. Analysis of the Drosophila Clock Promoter Reveals Heterogeneity in Expression between Subgroups of Central Oscillator Cells and Identifies a Novel Enhancer Region. J Biol Rhythms. 2009; 24:353–367. [PubMed: 19755581]
79. Zhao J, Kilman VL, Keegan KP, Peng P, Emery P, Rosbash M, Allada R. Drosophila Clock Can Generate Ectopic Circadian Clocks. Cell. 2003; 113:755–766. [PubMed: 12809606]
80. Kaneko H, Head LM, Ling J, Tang X, Liu Y, Hardin PE, Emery P, Hamada FN. Circadian rhythm of temperature preference and its neural control in Drosophila. Curr Biol. 2012; 22:1851–1857. [PubMed: 22981774]
81. Sprecher SG, Desplan C. Switch of rhodopsin expression in terminally differentiated Drosophila sensory neurons. Nature. 2008; 454:533–537. [PubMed: 18594514]
82. Mahr A, Aberle H. The expression pattern of the Drosophila vesicular glutamate transporter: a marker protein for motoneurons and glutamatergic centers in the brain. Gene Expr Patterns. 2006; 6:299–309. [PubMed: 16378756]
83. Bussell JJ, Yapici N, Zhang SX, Dickson BJ, Vosshall LB. Abdominal-B neurons control Drosophila virgin female receptivity. Curr Biol. 2014; 24:1584–1595. [PubMed: 24998527]
84. Diao F, Ironfield H, Luan H, Diao F, Shropshire WC, Ewer J, Marr E, Potter CJ, Landgraf M, White BH. Plug-and-Play Genetic Access to Drosophila Cell Types using Exchangeable Exon Cassettes. Cell Rep. 2015
85. Tanoue S, Krishnan P, Krishnan B, Dryer SE, Hardin PE. Circadian clocks in antennal neurons are necessary and sufficient for olfaction rhythms in Drosophila. Curr Biol. 2004; 14:638–649. [PubMed: 15084278]
86. Muskus MJ, Preuss F, Fan JY, Bjes ES, Price JL. Drosophila DBT Lacking Protein Kinase Activity Produces Long-Period and Arrhythmic Circadian Behavioral and Molecular Rhythms. Mol Cell Biol. 2007; 27:8049–8064. [PubMed: 17893330]
87. Smith EM, Lin JM, Meissner RA, Allada R. Dominant-negative CK2alpha induces potent effects on circadian rhythmicity. PLoS Genet. 2008; 4:e12. [PubMed: 18208335]
88. Han DD, Stein D, Stevens LM. Investigating the function of follicular subpopulations during Drosophila oogenesis through hormone-dependent enhancer-targeted cell ablation. Development. 2000; 127:573–583. [PubMed: 10631178]
89. Masuyama K, Zhang Y, Rao Y, Wang JW. Mapping neural circuits with activity-dependent nuclear import of a transcription factor. J Neurogenet. 2012; 26:89–102. [PubMed: 22236090]
90. Wagh DA, Rasse TM, Asan E, Hofbauer A, Schwenkert I, Dürrbeck H, Buchner S, Dabauvalle MC, Schmidt M, Qin G, et al. Bruchpilot, a protein with homology to ELKS/CAST, is required for structural integrity and function of synaptic active zones in Drosophila. Neuron. 2006; 49:833–844. [PubMed: 16543132]
91. Nicolai LJ, Ramaekers A, Raemaekers T, Drozdzecki A, Mauss AS, Yan J, Landgraf M, Annaert W, Hassan BA. Genetically encoded dendritic marker sheds light on neuronal connectivity in Drosophila. Proc Natl Acad Sci U S A. 2010; 107:20553–20558. [PubMed: 21059961]
92. Bourouis M. Targeted increase in shaggy activity levels blocks wingless signaling. Genesis. 2002; 34:99–102. [PubMed: 12324959]

93. Baines RA, Uhler JP, Thompson A, Sweeney ST, Bate M. Altered Electrical Properties in Drosophila Neurons Developing without Synaptic Transmission. J Neurosci. 2001; 21:1523–1531. [PubMed: 11222642]
94. Lin S, Huang Y, Lee T. Nuclear receptor unfulfilled regulates axonal guidance and cell identity of Drosophila mushroom body neurons. PLoS One. 2009; 4:e8392. [PubMed: 20027309]
95. Chen TW, Wardill TJ, Sun Y, Pulver SR, Renninger SL, Baohan A, Schreiter ER, Kerr RA, Orger MB, Jayaraman V, et al. Ultrasensitive fluorescent proteins for imaging neuronal activity. Nature. 2013; 499:295–300. [PubMed: 23868258]
96. Pfeiffer BD, Truman JW, Rubin GM. Using translational enhancers to increase transgene expression in Drosophila. Proc Natl Acad Sci U S A. 2012; 109:6626–6631. [PubMed: 22493255]
97. Shang Y, Griffith LC, Rosbash M. Light-arousal and circadian photoreception circuits intersect at the large PDF cells of the Drosophila brain. Proc Natl Acad Sci U S A. 2008; 105:19587–19594. [PubMed: 19060186]
98. Cavanaugh DJ, Geratowski JD, Wooltorton JR, Spaethling JM, Hector CE, Zheng X, Johnson EC, Eberwine JH, Sehgal A. Identification of a circadian output circuit for rest:activity rhythms in Drosophila. Cell. 2014; 157:689–701. [PubMed: 24766812]
99. Yao Z, Macara AM, Lelito KR, Minosyan TY, Shafer OT. Analysis of functional neuronal connectivity in the Drosophila brain. J Neurophysiol. 2012; 108:684–696. [PubMed: 22539819]
100. Chang HC, Newmyer SL, Hull MJ, Ebersold M, Schmid SL, Mellman I. Hsc70 is required for endocytosis and clathrin function in Drosophila. J Cell Biol. 2002; 159:477–487. [PubMed: 12427870]
101. Gong Z, Liu J, Guo C, Zhou Y, Teng Y, Liu L. Two pairs of neurons in the central brain control Drosophila innate light preference. Science. 2010; 330:499–502. [PubMed: 20966250]
102. Pichaud F, Desplan C. A new visualization approach for identifying mutations that affect differentiation and organization of the Drosophila ommatidia. Development. 2001; 128:815–826. [PubMed: 11222137]
103. Tanenhaus AK, Zhang J, Yin JC. In Vivo Circadian Oscillation of dCREB2 and NF-kappaB Activity in the Drosophila Nervous System. PLoS One. 2012; 7:e45130. [PubMed: 23077489]
104. Pfeiffer BD, Ngo TT, Hibbard KL, Murphy C, Jenett A, Truman JW, Rubin GM. Refinement of tools for targeted gene expression in Drosophila. Genetics. 2010; 186:735–755. [PubMed: 20697123]
105. Tataroglu O, Zhao X, Busza A, Ling J, O'Neill JS, Emery P. Calcium and SOL Protease Mediate Temperature Resetting of Circadian Clocks. Cell. 2015; 163:1214–1224. [PubMed: 26590423]
106. Wu Y, Cao G, Pavlicek B, Luo X, Nitabach MN. Phase Coupling of a Circadian Neuropeptide With Rest/Activity Rhythms Detected Using a Membrane-Tethered Spider Toxin. PLoS Biol. 2008; 6:e273. [PubMed: 18986214]
107. Venken KJ, Schulze KL, Haelterman NA, Pan H, He Y, Evans-Holm M, Carlson JW, Levis RW, Spradling AC, Hoskins RA, et al. MiMIC: a highly versatile transposon insertion resource for engineering Drosophila melanogaster genes. Nat Methods. 2011; 8:737–743. [PubMed: 21985007]
108. Klarsfeld A, Leloup JC, Rouyer F. Circadian rhythms of locomotor activity in *Drosophila*. Behav Processes. 2003; 64:161–175. [PubMed: 14556950]
109. Tajima Y, Salvaterra PM. Positive and negative feedback regulation of choline acetyltransferase mRNA levels in *Drosophila*: a study using temperature-sensitive mutants and embryo cell cultures. Brain Res Mol Brain Res. 1992; 13:213–221. [PubMed: 1317495]
110. Wang JW, Wong AM, Flores J, Vosshall LB, Axel R. Two-photon calcium imaging reveals an odor-evoked map of activity in the fly brain. Cell. 2003; 112:271–282. [PubMed: 12553914]
111. Shafer OT, Kim DJ, Dunbar-Yaffe R, Nikolaev VO, Lohse MJ, Taghert PH. Widespread receptivity to neuropeptide PDF throughout the neuronal circadian clock network of Drosophila revealed by real-time cyclic AMP imaging. Neuron. 2008; 58:223–237. [PubMed: 18439407]
112. Minocci D, Carbognin E, Murmu MS, Martin JR. In vivo functional calcium imaging of induced or spontaneous activity in the fly brain using a GFP-apoaequorin-based bioluminescent approach. Biochim Biophys Acta. 2013; 1833:1632–1640. [PubMed: 23287020]

HIGHLIGHTS

- The master pacemaker, LNv, *opportunistically* swaps its enslaved partner
- Light guides the choice of the best-adapted slave oscillator
- Morning (M) oscillators work *in series*, evening (E) ones work *in parallel*
- Bright light inhibits the DN1p E-oscillator output through visual inputs and PDF

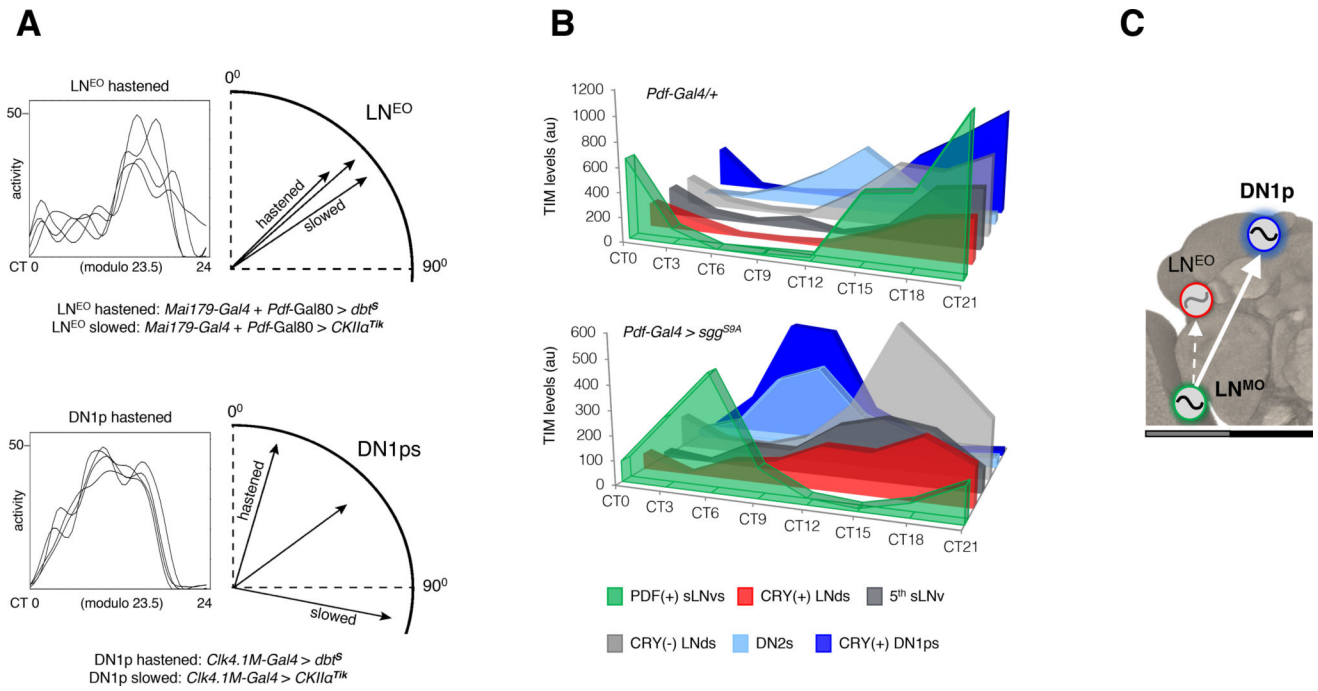

Figure 1. Coupling between the period-determining s-LNvs and phase-determining DN1ps is the main axis of network operation in the absence of light

(**A**) (Left) Representative waveforms of locomotor activity of a single fly over first 4 DD days are depicted in each box. (Right) Using the trough of the waveform as the phase-marker, phase vectors are constructed on circular plot on a 24-hour dial. Only the relevant part of the plot is depicted here for flies in which either LN^{EO} or DN1p oscillator underwent speed change. Unlike the LN^{EO}, DN1p oscillator triggered dramatic phase changes (significant at α=0.05 by Watson's non-parametric two-sample U^2 statistic) upon alteration of its endogenous pace. (see Table 1) (**B**) Immunostaining of TIM protein at eight different time-points on the fourth day of DD shows oscillations for each neuronal group. Synchrony across subsets (except the DN2s) occurred in *Pdf-Gal4/+* flies but was dismantled in *Pdf-Gal4 > sgg*^{S9A} (faster pace of the PDF+ LNv oscillator) flies. Comparison of the TIM cycling profiles of different subgroups of PDF(−) oscillators of *Pdf-Gal4 > sgg*^{S9A} flies reveals that no other subgroup within the PDF(−) clock neurons could follow the PDF(+) s-LNvs as much as the CRY(+) DN1ps did (see Figure S2). (**C**) The model shows the dominant axis of coupling in DD within the multi-oscillator network. See also Figure S1.

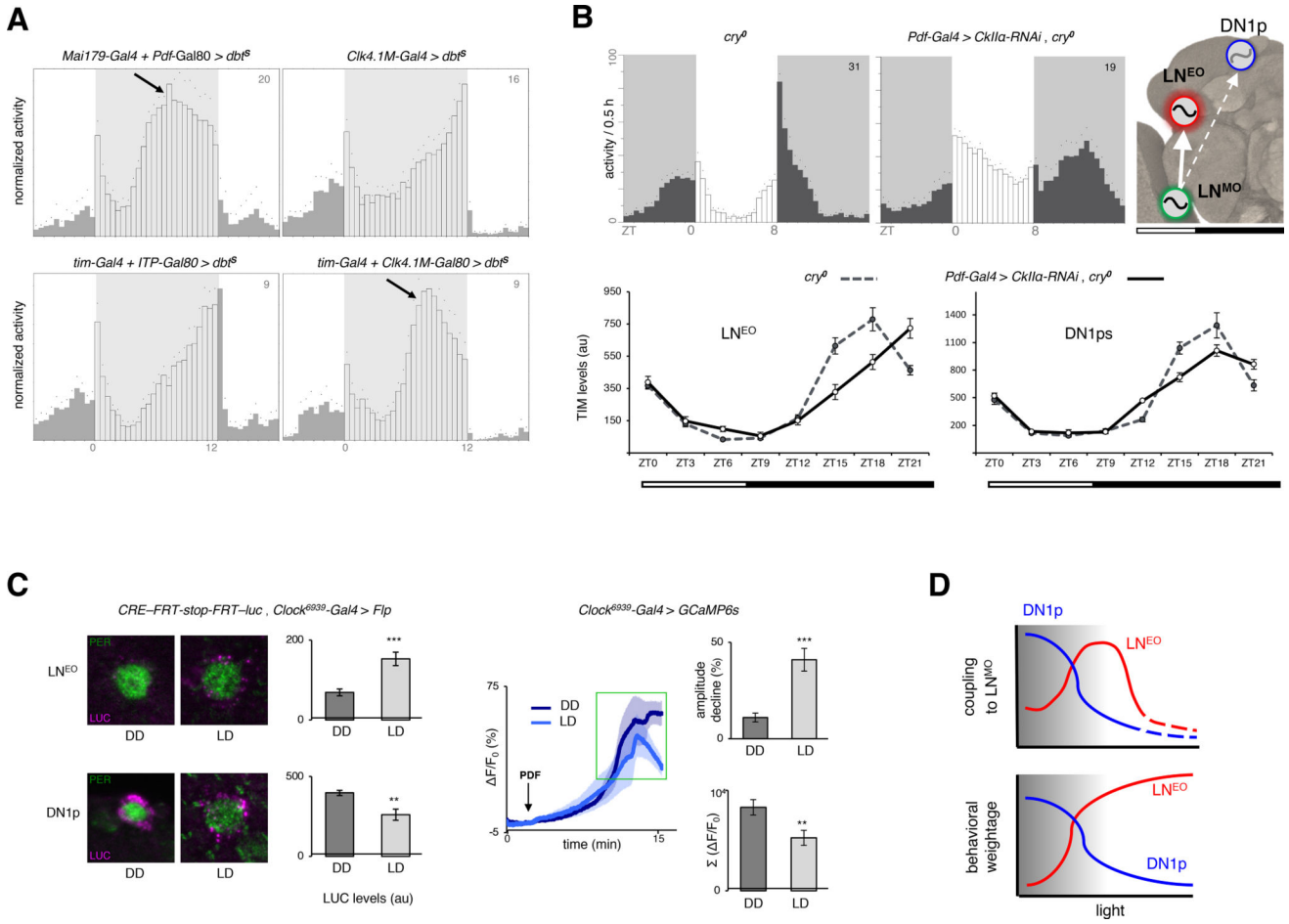

Figure 2. Opportunistic swap of the coupled partner in the presence of light

(**A**) DBT^{S}-mediated acceleration of the LN^{EO} and DN1p oscillators, or all oscillators except LN^{EO}/DN1p under 12:12 low-light LD cycles (See Figure S3 for quantifications). Low light is indicated by grey shading on daytime. (**B**) (Upper panel) Under short photoperiod (8:16) LD cycles, the LN^{MO} was decelerated (30h period in DD) through knockdown of *CkIIα* in *cry*$^{-/-}$ background, and the resulting delay in the evening output produced by the PDF(−) oscillators was assessed. (Lower panel). Differential changes in the clock program of the LN^{EO} (left) and DN1p (right) oscillators under such conditions, with the former showing stronger coupling to the LN^{MO}. Each point in the line graph represents the average of at least 30 cells from at least 10 brain hemispheres. Cosinor analysis on the TIM cycling pattern reveals a >1.5 hr phase-delay in LN^{EO} and a <0.5 h delay in DN1p, enforced by the slower-running LN^{MO}. The model shows the dominant axis of coupling under LD cycles. (**C**) (Left panel) CRE-*luc* staining in LN^{EO} is higher under LD (day 4, ZT3–4), while higher in DN1ps under DD (day 4, CT3–4). In the bar graph showing LUC staining intensity, *n* from left to right are 18, 8 for the LN^{EO} and 51, 30 for the DN1ps. (Right panel) GCaMP6s fluorescence in DN1ps after bath-application of 30μM PDF under DD and LD cycles. The traces are averages of 5 representative responses. *n*=24 for the two bar plots, recorded during ZT/CT6–9 on day 4–5 of LD and DD. **p<0.01, *** p<0.0001 after unpaired two-tailed Student's *t*-test. (**D**) The working model posits that with increased light, the LN^{MO} switches

coupling from DN1ps to LN^{EO}, thereby optimizing its influence on the behavioral phase set by the PDF(−) oscillators. In excess light, the LN^{EO} takes the lead for controlling behavior and liberates from the pacesetting influence of the LN^{MO} (see Table S1). The number on the top-right corner of the activity plots shows the sample size of analyzed flies for a single run of the behavioral experiment. Error bars represent the s.e.m.

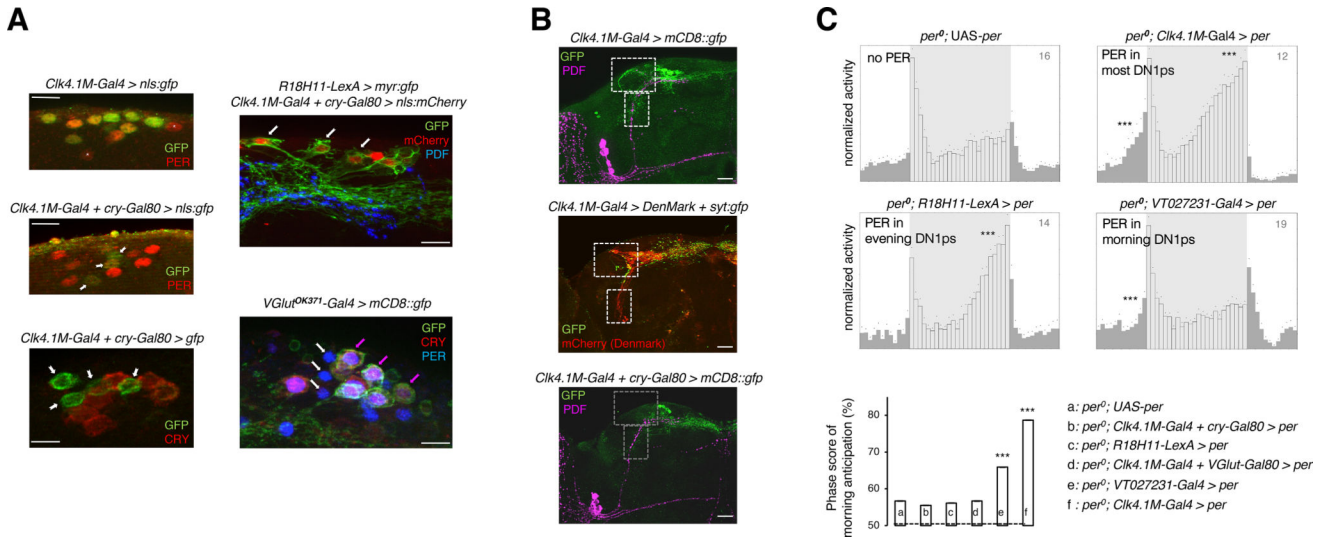

Figure 3. Functional subdivision of the DN1p cluster

(**A**) (Left panel) About 4–5 DN1ps lacking CRY protein expression, examples of which are marked with white arrow, were labelled with cytosolic-GFP and nls-GFP driven by the intersectional driver *Clk4.1M-Gal4 + cry-Gal80. Clk4.1M-Gal4* alone drove GFP expression in about 10 of the DN1ps including all the 6 CRY(+) cells. The few DN1p neurons that were not labeled by the *Clk4.1M-Gal4* driver are marked with white asterisks. (Right panel, top) Expression pattern of the DN1p-restricted *R18H11-LexA* which drives evening anticipation like the CRY(−) DN1ps, has extensive overlap with the latter subgroup, as marked with white arrows. (Right panel, bottom) Most of the CRY(+) DN1ps co-expressed *VGlut^{OK371}*-Gal4-driven CD8::GFP demonstrating the convergence of *VGlut* and *cry* expression in the morning subset of the DN1ps, marked with colored arrows. Evening DN1p cells that were both *VGlut(−)* as well as CRY(−), are marked with white arrows (See Figure S4 for further characterization of the subgroups). All PER stainings were carried out at ZT0–2. (**B**) Projection patterns of the *Clk4.1M-Gal4*-expressing DN1ps (top) with dendritic arborization recognized by the DenMark marker (middle) labeled with white boxes. The CRY(−) evening DN1ps (bottom) lack the afferent fibers in the lateral and ventral protocerebrum. (**C**) Averaged locomotor activity profiles over 24-hour LD days reveal that an oscillator in the *R18H11-LexA* labeled, CRY(−) or *VGlut(−)* DN1ps (see Figure S4) was unable to elicit morning anticipation but could evoke evening anticipation. Another subset of the DN1p oscillator, identified by the Gal4 line *VT027231* covering the *VGlut(+)* DN1ps (Figure S4), was sufficient for morning anticipation but not for evening anticipation. Significance of anticipatory activity was ascertained by Spearman's non-parametric rank-correlation test (to measure the strength and direction of putatively monotonic association between the ranked variables activity-count and time-interval); **p<0.01, *** p<0.001. The column chart depicts mean ± s.e.m of the 3h/6h activity ratio prior to the light-on transition, *i.e.*, an estimate of the amplitude of morning anticipation. *** p<0.0001, by one-way ANOVA followed by Tukey's post-hoc test. Light intensity during the 12 hour of photoperiod was 50 lux, for all the eductions shown.

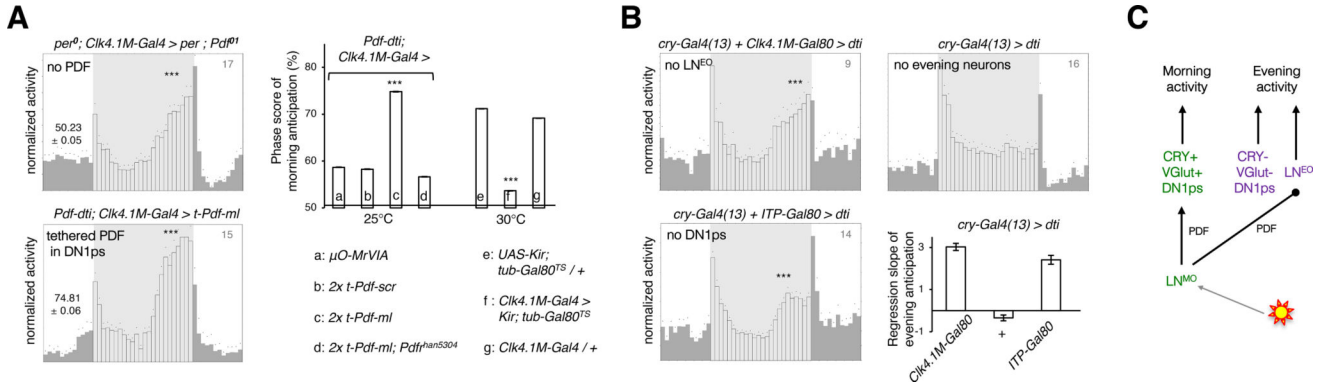

Figure 4. Distinct logic of circuit organization for morning and evening activity

(**A**) (Left panel) Morning and evening anticipatory activity were differentially affected when the DN1p clock had no access to the PDF neuropeptide. The averaged activity profile showed no significant morning anticipation (p=0.87), but persistent evening anticipation (*** p<0.0001) based on Spearman's non-parametric rank-correlation test. Restoring PDF signaling onto the DN1ps of LNv-less flies brought back the morning peak (*** p<0.0001). (Right panel) Impact on morning anticipation of expressing membrane-tethered PDF, *i.e., t*-PDF_{ML}, or its scrambled analog, *i.e., scr*-PDF, or an inactive control peptide *μO*-MrVIA, in the DN1ps of LNv-less flies *(Pdf-dti)* in the absence or presence of PDFR or silencing the DN1ps by adult-specific expression of the Kir2.1 channel. For the column chart, *n* from left to right are 16, 16, 15, 9, 15, 11, and 16. *** p<0.0001, by one-way ANOVA followed by Tukey's post-hoc test. (**B**) Evening activity in flies that lack the LN^{EO} and/or the DN1ps (see Figure S4). The column plot shows mean ± s.e.m of the slope of a linear regression fitted on the last four hours of activity prior to the evening peak, which is a measure of the strength of the evening peak. Light intensity during the 12 hours of photoperiod was 50 lux, for all the eductions shown. (**C**) Scheme showing the LN^{MO} and CRY(+) $DN1p^{MO}$ working in series to build the morning activity, while the LN^{EO} and CRY(−) $DN1p^{EO}$ working in parallel to produce the evening activity. PDF is required for morning activity and influences the phasing of LN^{EO} generated evening activity. The effect of genotype was significant by one-way ANOVA at α=0.0001. The number on the top-right corner of the activity plots shows the sample size of analyzed flies for a single run of the behavioral experiment. Error bars represent the s.e.m.

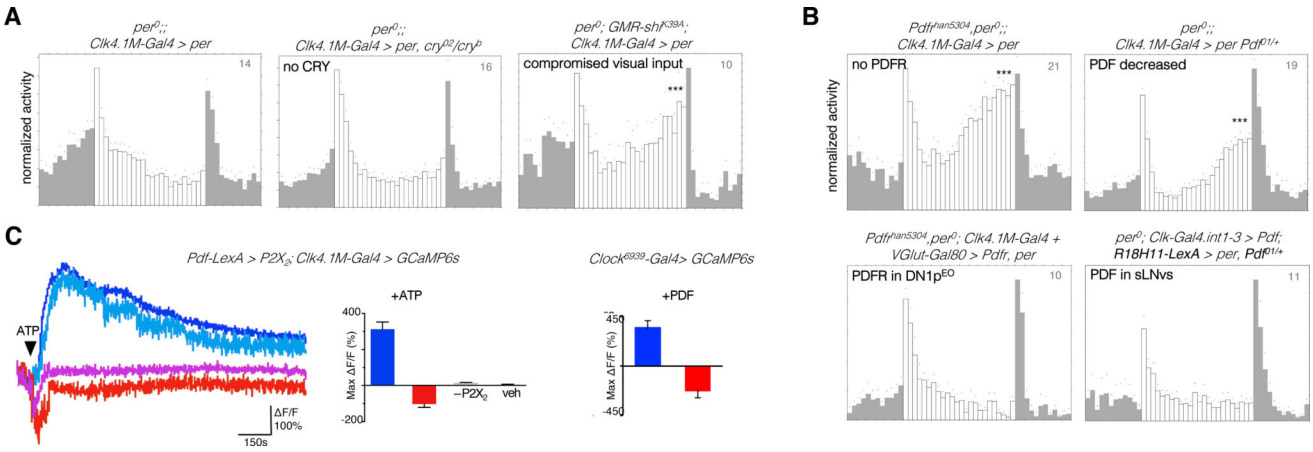

Figure 5. Direct gating of the DN1p^{EO} output by visual light inputs and PDF

Evening peak under high light (1000 lux) conditions in flies with working oscillator confined to the DN1ps (See Figure S5 for quantifications). Status of the DN1p-made evening peak when (**A**) different modes of light input were compromised (**B**) PDF/PDFR signaling was manipulated. (**C**) Different patterns of calcium response in DN1p cells on activation of the LNv neurons (left), and bath application of 0.1mM PDF (right). The representative traces depict signal changes from four different cells of a single brain. Note the presence of a group, marked by shades of red, mounting a response consistent with physiological inhibition. 5mM ATP causes significant ($p<0.05$ by Kruskal-Wallis multiple comparisons test followed by Dunn's post-hoc analysis) increase (bluish hues) or decrease (reddish hues) in GCaMP6 signal, compared to $P2X_2$-non-expressing ($-P2X_2$) and vehicle (veh) controls. 89 of the 131 recorded DN1p*s* elicited excitatory response, while 38 of them elicited inhibitory response. n=14,14,4,4 brains for the ATP/$P2X_2$ bar plot (left) and n=8,8 for the PDF bar plot (right). Recordings were carried out at ZT6–9 (See Figure S6 for bioluminescence-based live imaging of intracellular calcium in DN1p).

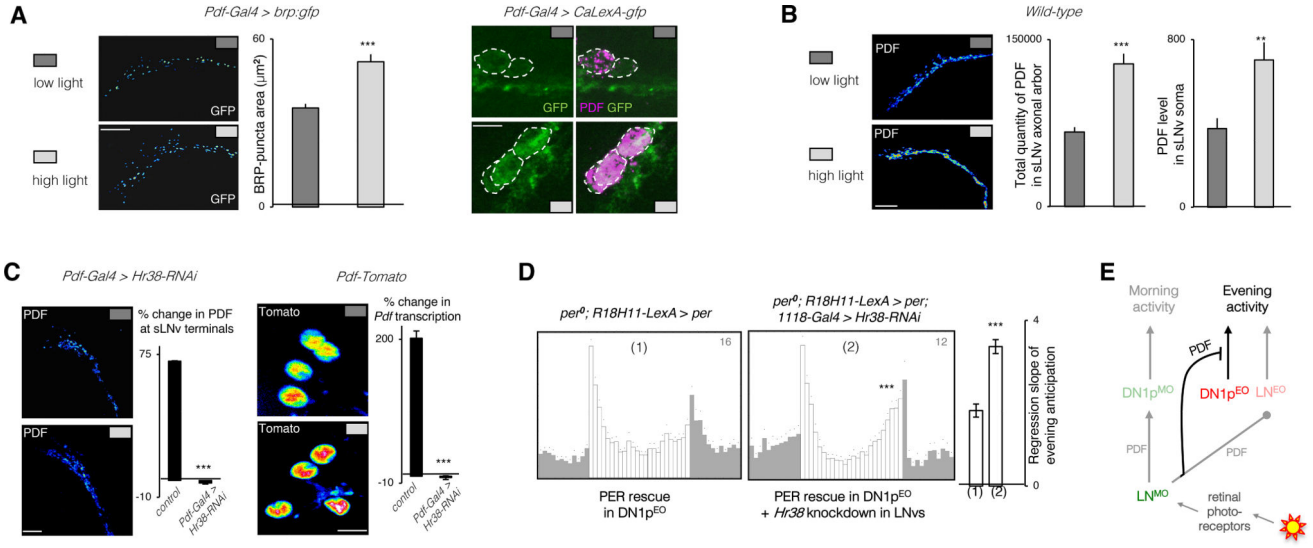

Figure 6. Ambient light-intensity is encoded in Hr38-dependent *Pdf* transcription

(**A**) Expression of the active-zone marker BRP (BRUCHPILOT) (left) or the transcription-based CaLexA-GFP reporter (right) in the s-LNvs under low and high light intensities at ZT13–14. (**B**) Comparison of the levels of PDF peptide in the axon terminals and cell bodies of the s-LNvs under different light intensities at ZT13–14 indicates that the physiological output from the s-LNv neurons is promoted by high light. The column plot shows mean ± s.e.m of the slope of a linear regression fitted on the last four hours of activity prior to the evening peak. (**C**) Light-induction of PDF levels in s-LNv terminals in wild type flies or flies with downregulated *Hr38* in the LNvs (left). Light-induction of a Tomato-based transcriptional reporter of *Pdf* in the s-LNv nuclei of wild-type flies and flies with downregulated *Hr38* in the LNvs. % changes are from low-to-high light. Labelings are done at ZT13–14. (**D**) High light LD activity profiles of flies with a functional oscillator in the evening DN1ps in a wild type (1) or downregulated *Hr38* (2) background. (**E**) Scheme showing that visually estimated ambient light-intensity changes PDF levels in the s-LNv cells. PDF suppresses the output of the CRY(−) DN1ps that produce evening activity. Each column in immunostaining experiments of (d), (e), and (f) represents mean ± s.e.m. of at least 8 brain hemispheres. *** p<0.0001 by unpaired two-tailed Student's *t*-test, Fisher's exact test was used for comparing % changes in (f). Representative stained images are pseudocolored, such that red-shifted colors denote stronger signal intensity. The number on the top-right corner of the activity plots shows the sample size of analyzed flies for a single run of the behavioral experiment. See also Figure S6.

Table 1

Analyses of the phase of the free-running rhythms under constant darkness (DD)

Genotypes with a faster or slower oscillator in defined clusters of clock neurons are separated: DN1p on the top, LN^{EO} in the middle, and LN^{MO} at the bottom. N: number of flies. Phase and Power are defined in the STAR Methods.

Genotype	Phase				Period ± s.e.m	% Rhythmic	Power ± s.e.m	N
	Valley ± 95% CI	*p*	Conc.	*p*				
Clk4.1M-Gal4/+	3.4 ± 1.1	<.001	.862	<.001	24.0 ± .12	93.8	85.3± 8.85	16
UAS-dbt^{S}/+	3.4 ± 1.7	.003	.805	.001	23.5 ± .05	76.9	80.2 ± 12.75	13
Clk4.1M-Gal4/UAS-dbt^{S}	0.8 ± 0.7	<.001	.935	<.001	23.7 ± .07	100	98.3 ± 7.95	17
UAS-CkIIα^{Tik}/+	3.8 ± 1.2	<.001	.753	<.001	23.8 ± .08	100	86.3 ± 7.08	16
Clk4.1M-Gal4/UAS-CkIIα^{Tik}	7.2 ± 1.7	<.001	.693	<.001	23.9 ± .07	69.6	86.2 ± 8.11	23
Mai179-Gal4/+; Pdf-Gal80/+	3.0 ± 1.9	.004	.765	.003	23.1 ± .16	60	54.2 ± 7.11	15
Mai179-Gal4/+; Pdf-Gal80/UAS-dbt^{S}	2.2 ± 1.1	<.001	.868	<.001	23.4 ± .16	68.4	36.2 ± 2.86	19
Mai179-Gal4/+; Pdf-Gal80/UAS-CkIIα^{Tik}	3.9 ± 1.9	<.001	.697	<.001	23.5 ± .10	82.4	64.8 ± 6.86	17
cry-Gal4(19)/+; Pdf-Gal80/+	3.3 ± 1.3	.031	.925	.002	23.4 ± .08	54.5	58.1 ± 8.76	11
cry-Gal4(19)/+; Pdf-Gal80/UAS-dbt^{S}	3.3 ± 1.1	<.001	.805	<.001	23.4 ± .07	100	95.5 ± 9.29	17
cry-Gal4(19)/+; Pdf-Gal80/UAS-CkIIα^{Tik}	3.8 ± 3.3	.035	.571	.046	23.3 ± .12	42.9	54.0 ± 11.78	21
Pdf-Gal4/+	4.1 ± 1.2	<.001	.846	<.001	24.2 ± .10	57.1	67.9 ± 14.83	21
UAS-sgg^{S9A}/+	4.2 ± 2.2	<.001	.602	.002	23.5 ± .03	100	73.1 ± 6.13	16
Pdf-Gal4/UAS-sgg^{S9A}	2.2 ± 0.9	<.001	.897	<.001	22.8 ± .14	63.2	43.3 ± 4.34	19
UAS-CkIIα-RNAi/+	4.2 ± 0.8	<.001	.946	<.001	23.5 ± .03	100	80.0 ± 5.17	15
Pdf-Gal4/+; UAS-CkIIα-RNAi/+	6.7 ± 1.0	.004	.926	<.001	25.7 ± .28	64.3	49.3 ± 6.57	14

KEY RESOURCES TABLE

REAGENT or RESOURCE	SOURCE	IDENTIFIER
Antibodies		
Guinea-Pig polyclonal anti-CRY	Joel Levine, University of Toronto	N/A
Rabbit polyclonal anti-PER	[69]	PER-12.1, PER-13.1
Rat polyclonal anti-TIM	[70]	N/A
Mouse monoclonal anti-PDF	DSHB	PDF C7-c; RRID: AB_760350, AB_2315084
Rabbit polyclonal anti-PDF	[71]	N/A
Guinea-pig polyclonal anti-proPDF (PAP)	[62]	N/A
Rabbit polyclonal anti-DsRed	Clontech	Cat#632496; RRID:AB_10013483
Chicken polyclonal anti-GFP	ThermoFisher	Cat#A10262; RRID: AB_2534023
Rabbit polyclonal anti-GFP	ThermoFisher	Cat#A11122; RRID: AB_221569
Mouse monoclonal anti-GFP	ThermoFisher	Cat#A11120; RRID: AB_221568
Mouse monoclonal anti-LUC-Y	ThermoFisher	Cat#MA1-80225; RRID: AB_934495
Chemicals, Peptides, and Recombinant Proteins		
Drosophila pigment dispersing factor (PDF)	PolyPeptide Group	N/A
Experimental Models: Organisms/Strains		
D. mel: cry^{b}	[72]	N/A
D. mel: cry^{0}	[73]	N/A
D. mel: Pdf^{01}	[62]	BDSC#26654
D. mel: Pdfr^{han5304}	[74]	BDSC#33068
D. mel: per^{0}	[75]	N/A
D. mel: Pdf-Gal4	[62]	BDSC#6900
D. mel: Clk4.1M-Gal4 (±10 DN1p)	[18]	BDSC#36316
D. mel: Mai179-Gal4 (most LNv, 3 LNd, 2 DN1a)	[76]	N/A
D. mel: tim(UAS)-Gal4 (all clock neurons)	[77]	N/A
D. mel: Clock^{6939}-Gal4 (all clock neurons)	[78]	N/A
D. mel: cry-Gal4(19) (all LNv, ±3 LNd, 2 DN1a)	[15]	N/A
D. mel: cry-Gal4(13) (all LNs, 2 DN1a, ±9 DN1p)	[79]	N/A

REAGENT or RESOURCE	SOURCE	IDENTIFIER
D. mel: Clk-int1-3-Gal4(9M) (most s-LNv, ±1 DN2)	[80]	BDSC#41810
D. mel: Gal1118 (all LNv, ±1 LNd)	[32]	N/A
D. mel: Rh5-Gal4 (RH5 expressing photoreceptors)	[81]	N/A
D. mel: OK371(VGlut)-Gal4 (glutamatergic neurons)	[82]	BDSC#26160
D. mel: VT027231-Gal4 (±7 DN1p, few DN3)	VDRC	v205530
D. mel: Pdf-Gal80	[25]	N/A
D. mel: cry-Gal80	[25]	N/A
D. mel: VGlut-Gal80	[83]	BDSC#58448
D. mel: ITP-Gal80	This paper	N/A
D. mel: Clk4.1M-Gal80	This paper	N/A
D. mel: VGlut^{MI04979}-Gal80	[84]	BDSC#60316
D. mel: UAS-per16	Blanchardon et al., 2001, #2473]	N/A
D. mel: UAS-cyc^{DN}	[85]	BDSC#36317
D. mel: UAS-CkIIα-RNAi	NIG-FLY	17520-R2
D. mel: UAS-dbt^{S}	[86]	N/A
D. mel: UAS-CkIIα^{Tik}	[87]	BDSC#24624
D. mel: UAS-dti	[88]	BDSC#25039
D. mel: UAS-CaLexA; LexAop-GFP	[89]	BDSC#66542
D. mel: UAS-brp:gfp	[90]	BDSC#36292
D. mel: UAS-DenMark,UAS-syt:gfp	[91]	BDSC#33065
D. mel: UAS-sgg^{S9A}	[92]	BDSC#5255
D. mel: UAS-Kir	[93]	BDSC#6596
D. mel: UAS-Hr38-miRNA	[94]	BDSC#44396
D. mel: UAS-GCaMP6s	[95]	BDSC#42746
D. mel: 20xUAS-aeq:gfp	[47]	N/A
D. mel: 10xUAS-cd8:gfp	[96]	BDSC#32185
D. mel: UAS-gfp^{S65T}	FlyBase	BDSC#1521
D. mel: UAS-nls:gfp	FlyBase	BDSC#4775
D. mel: UAS-nls:mCherry	FlyBase	BDSC#38425

REAGENT or RESOURCE	SOURCE	IDENTIFIER
D. mel: UAS-tPDFscr	[37]	N/A
D. mel: UAS-tPDFml	[37]	N/A
D. mel: UAS-t-μO-MrVIA	[37]	N/A
D. mel: Pdf-LexA	[97]	N/A
D. mel: Clk4.1M-LexA	[98]	N/A
D. mel: GMR18H11-LexA	Janelia Farm	BDSC#52535
D. mel: LexAop-P2X$_2$	[99]	BDSC#76030
D. mel: LexAop-per	This paper	N/A
D. mel: LexAop-myr:gfp	[96]	BDSC#32209
D. mel: GMR-shi^{K39A}	[100]	BDSC#7115
D. mel: Pdf-DTI	[101]	N/A
D. mel: Rh6-GFP	[102]	N/A
D. mel: UAS-Flp; CRE-F-luc	[103]	N/A
D. mel: Pdf-nls.Tomato:PEST	[55]	N/A
Oligonucleotides		
Primer: *per*-forward 5'-aaactcgagACTAGTCAACCAACTGGGCAAG-3'	This paper	N/A
Primer: *per*-reverse 5'aaatctagaGAAGAACTTGAAGGGAATGGAA-3'	This paper	N/A
Recombinant DNA		
pJFRC-19	[104]	Addgene plasmid #26224
pBS-KS-attB1-2-GT-SA-Flpo-SV40	DGRC	Barcode #1326
Software and Algorithms		
R	Version 3.4.4	https://www.r-project.org/
Prism 7	GraphPad	https://www.graphpad.com/scientific-software/prism/
FaasX	Michel Boudinot, François Rouyer, Université Paris Sud, CNRS, Université Paris-Saclay	http://neuro-psi.cnrs.fr/spip.php?article298&lang=en
Zen 2	Zeiss	https://www.zeiss.com/microscopy/int/products/microscope-software/zen-2-core.html
Fiji	ImageJ, NIH	https://fiji.sc/